

Research Article

Investigating a Hypothetical Semiconductor Laser Bar Using a Laser Diode Simulation/Emulation Tool Using Random Levels of Defects

^{1,2}C.K. Amuzuvi and ¹J.C. Attachie

¹Department of Electrical and Electronic Engineering, University of Mines and Technology, Tarkwa, Ghana

²Photonic and Radio Frequency Engineering Group (PRFEG), Electrical Systems and Optics Research Division, Faculty of Engineering, University of Nottingham, Nottingham, NG7 2RD, United Kingdom

Abstract: In this study, *Barlase*, a semiconductor laser diode emulation tool, is used to emulate the by-emitter degradation of high power semiconductor laser diodes. *Barlase* is a software that uses a LabView control interface. We have demonstrated how *Barlase* works using a hypothetical laser diode bar (multiple emitters) to validate the usefulness of the tool. A scenario using the hypothetical bar was investigated to demonstrate *Barlase* as follows: random low-level of defects distributed across the bar. The results of the simulation show the successful implementation of *Barlase* in the by-emitter analysis of laser diodes.

Keywords: Band gap energy, by-emitter, defect, degradation, emitter, nonradiative recombination, quantum well, slope efficiency, temperature, threshold current

INTRODUCTION

Progress in the development of high-power laser bars is due to their high demand and their improved reliability and durability. This has warranted the widespread usage (Steele, 2008) of such devices in recent times. Other applications have emerged which include: light detection and ranging and free space optical communications (Chazan *et al.*, 1998) apart from the traditional applications of laser diodes such as pumping solid-state lasers, material processing (Schulz and Poprawe, 2000), printing, medicine and entertainment.

The simulation tool, *Speclase*, which is a 2.5 D spectral laser model, the full details of which have been published elsewhere Lim *et al.* (2009) and Lim *et al.* (2007), gave rise to *Barlase* (Amuzuvi and Attachie, 2013). This study will discuss how a LabView control interface is used to communicate between *Speclase* and *Barlase* for by-emitter analysis of a laser bar.

The emulation tool presents an attempt to understand further, the by-emitter degradation analysis technique developed over recent years by Xia *et al.* (2002), Tomm *et al.* (2002), Bull *et al.* (2005), Lim *et al.* (2005) and Bream *et al.* (2006). This study also describes and explores the use of *Barlase* to simulate lasers at the multi-emitter level of operation.

MATERIALS AND METHODS

The simulation tool (*Speclase*) was designed for a single emitter. Since bars are made up of multiple emitters, there was a need to find an innovative way to include the interactions between individual emitters within the bar. This gave rise to the *Barlase* concept (Fig. 1), where a bar is considered as a monolithic block of multiple emitters connected in parallel with each other with a common voltage connected across them. The representation of an eight emitter laser bar used in the simulations is shown in Fig. 2.

Each emitter is biased with a common voltage, but the emitter currents and powers change depending on the details of the individual emitters and their environment. *Barlase* is also able to emulate different modes of operation (i.e., constant current or constant power). *Barlase* simulates the laser bar by calling multiple instances of *Speclase*.

A multi-emitter simulation scenario investigated was the introduction of a random low level of defects across the emitters in the bar. From the single emitter simulations (Amuzuvi and Attachie, 2013), it was observed that increasing the QW trap density from 2×10^{15} to $2 \times 10^{16} \text{ cm}^{-3}$ caused a reduction in the output power of a few percent. Experimentally, the power between emitters in a new laser bar varies by <5%. The randomized defect level for each emitter was therefore determined by generating a random number between 0

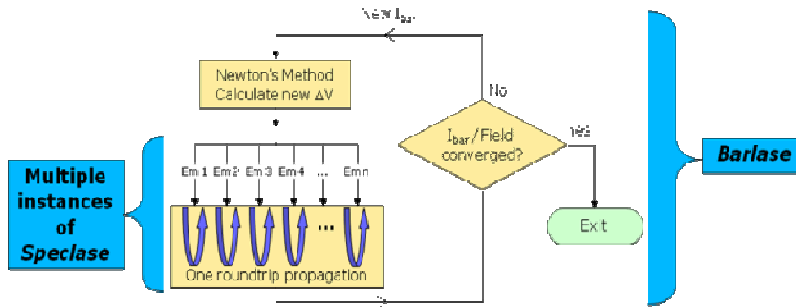


Fig. 1: Flow chart showing the communication between *Speclase* and *Barlase*

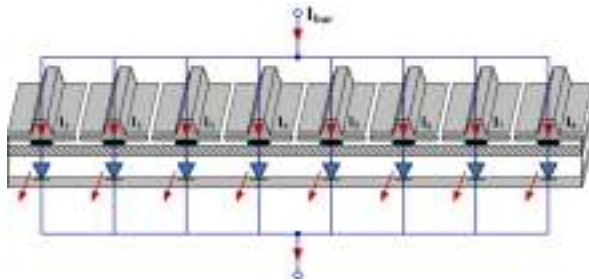


Fig. 2: The representation of an eight emitter laser bar

Table 1: Values of QW trap densities assigned to each emitter in the bar

Emitter number	Trap density (cm ⁻³)
1	6.06 × 10 ¹⁴
2	1.88 × 10 ¹⁶
3	4.83 × 10 ¹⁵
4	1.22 × 10 ¹⁶
5	9.73 × 10 ¹⁵
6	1.13 × 10 ¹⁶
7	1.05 × 10 ¹⁶
8	1.31 × 10 ¹⁶

and 1 and multiplying this by $2 \times 10^{16} \text{ cm}^{-3}$ (Table 1). These new QW trap densities were then used in the simulation input files for each emitter. Multi-emitter simulations were carried out in constant current mode for bar currents of 2, 4, 6, 8 and 10 A, respectively.

RESULTS AND DISCUSSION

Figure 3a and b shows the P-I characteristics of the bar and the P-I characteristics of each of the individual emitters. The threshold current and slope efficiency for the bar are also shown as legend in Fig. 3a. The equivalent bar current-voltage characteristic is shown in Fig. 4a and the emitter powers versus voltage are shown in Fig. 4b. The threshold current and slope efficiency were calculated for each emitter from the emitter P-I curves of Fig. 3b. These quantities are plotted as a function of emitter number in Fig. 5. As expected, the threshold current increases and the slope efficiency decreases for emitters with a higher trap density. There is up to a 10% variation in the threshold currents in this example, whilst the variation in slope efficiencies is <0.3%. Figure 5 also shows the simulated values for the “apparent” threshold current and “apparent” slope

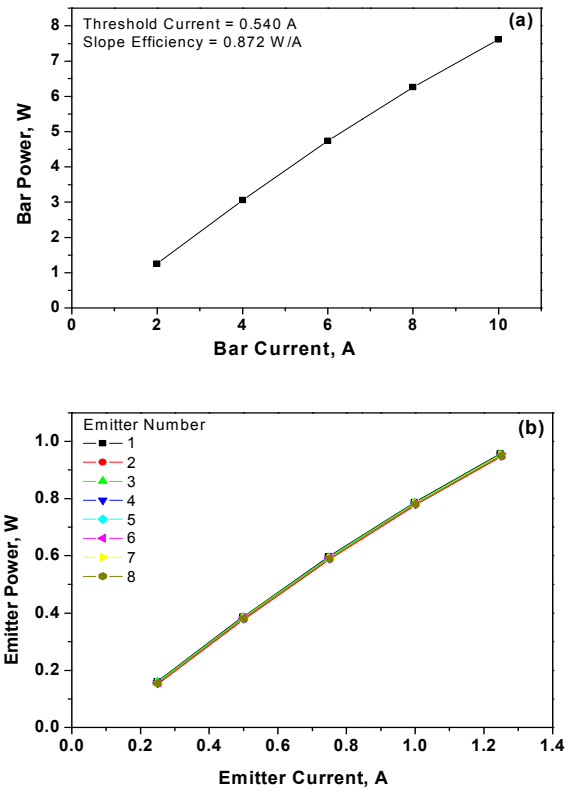


Fig. 3: (a) Power-current characteristics of the full bar, (b) of the individual emitters

efficiency of each emitter, since the actual threshold currents and slope efficiencies of the individual emitters in a laser bar cannot be measured. The apparent threshold current and apparent slope efficiency can be measured experimentally, but cannot be directly compared with their traditional counterparts. (They are defined similarly to the threshold current and slope efficiency, but use the individual emitter power and the total bar current).

Figure 6 shows the distribution of current, power and maximum QW temperature for each emitter across the bar for a total bar current of 2 A. Figure 7 shows the same quantities for a total bar current of 10 A. From the graphs in Fig. 6 and 7, a correlation can be seen between the currents, powers and maximum QW

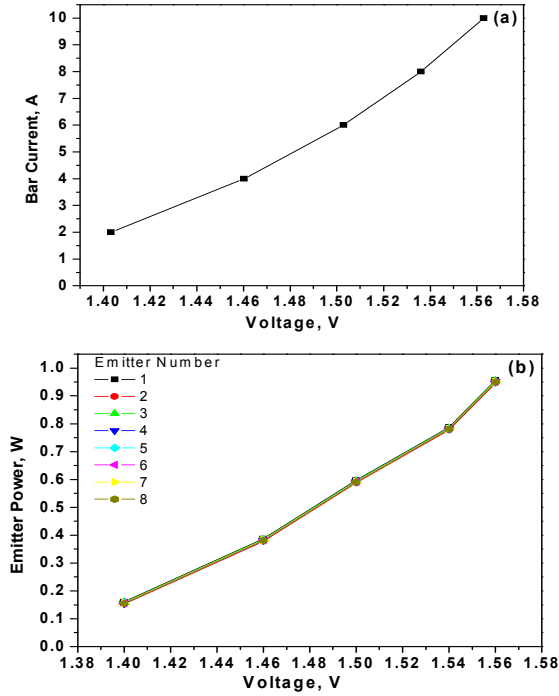


Fig. 4: (a) Current-voltage characteristics of the bar, (b) power-voltage characteristics of the individual emitters

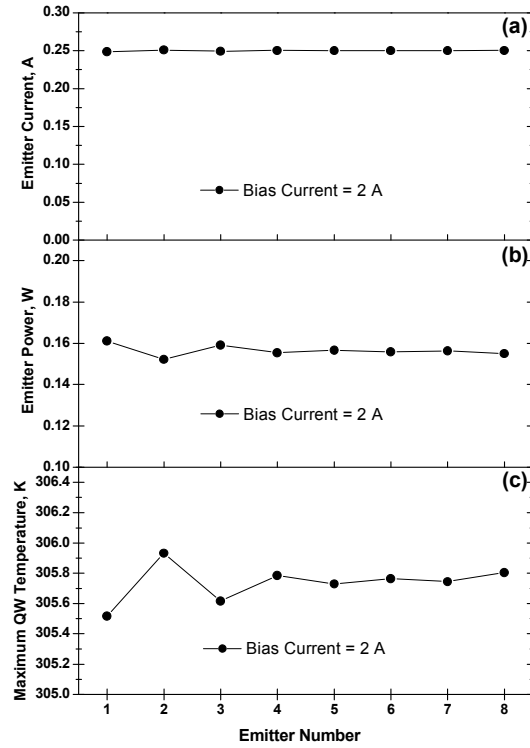


Fig. 6: (a) Distribution of the emitter currents, (b) emitter powers and (c) maximum emitter QW temperatures across the bar at a total bar bias current of 2 A

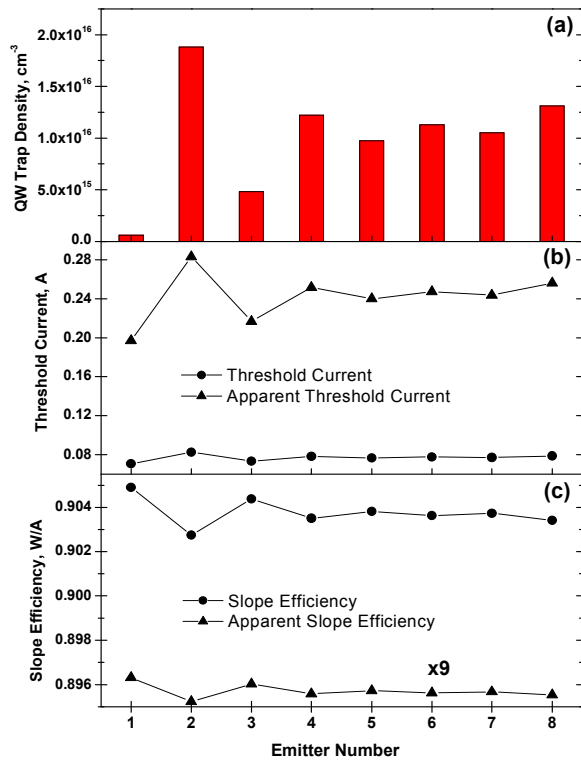


Fig. 5: QW trap densities assigned to each emitter, (b) variation of apparent threshold/threshold current and (c) apparent slope/slope efficiency of individual emitters

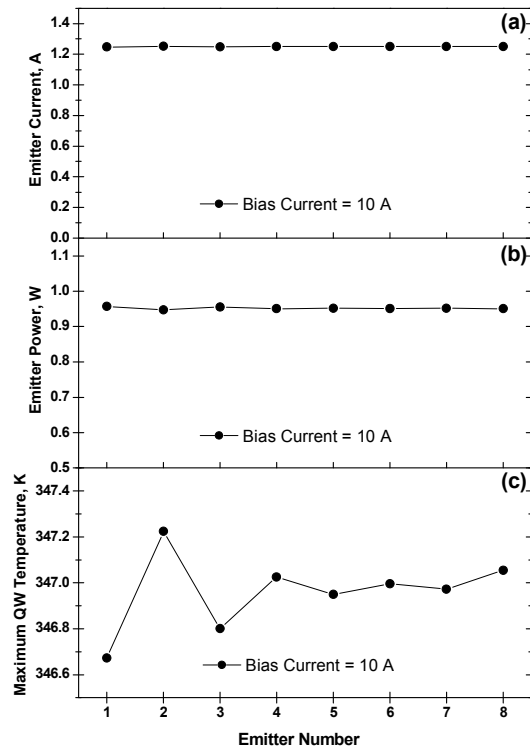


Fig. 7: (a) Distribution of the emitter currents, (b) emitter powers and (c) maximum emitter QW temperatures across the bar at a total bar bias current of 10 A

temperatures of the individual emitters. The emitters with the highest levels of defects draw more of the total bar current (meaning there is less available for emitters with fewer defects), but emit less power because of the higher level of nonradioactive recombination. Consequently, these emitters are also hotter. The variations in the emitter current and power across the bar are up to 0.3 and 1.0%, respectively. The variation in the maximum QW temperature of the emitters is ~0.5 K.

CONCLUSION

The scenario investigated using multi-emitter simulations show that variations in the operating conditions and environment of the individual emitters also affect the performance of the other emitters and of the bar as a whole.

It must be remembered that this scenario is for devices at the start of the aging process. When all of the relevant effects are combined and allowed to interact over time, high levels of defects are expected to play a more important role. Indeed, it is well known that the nucleation, propagation and growth of defects increase with temperature. Thus, the rates of defect generation and propagation within emitters are inextricably linked to the temperature profile. Finally, it was shown that the experimentally measurable “apparent” threshold current and “apparent” slope efficiency of the emitters change in the opposite direction to their actual threshold current and slope efficiency. This is caused by current competition resulting from a reduction in the turn-on voltage, which is caused by local temperature and/or strain-induced changes in the band gap energy.

ACKNOWLEDGMENT

CKA thanks the University of Mines and Technology, Tarkwa, Ghana and the GetFund for their support.

REFERENCES

Amuzuvi, C.K. and J.C. Attachie, 2013. Describing a laser diode emulation tool using single emitter simulation results. *Res. J. Appl. Sci. Eng. Technol.*, 5(4): 1358-1361.

Bream, P.J., J.J. Lim, S. Bull, A.V. Andrianov, S. Sujecki and E.C. Larkins, 2006. The impact of nonequilibrium gain in a spectral laser diode model. *Opt. Quant. Electron.*, 38(12-14): 1019-1027.

Bull, S., J.W. Tomm, M. Oudart, J. Nagle, C. Scholz, K. Boucke, I. Harrison and E.C. Larkins, 2005. By-emitter degradation analysis of high-power laser bars. *J. Appl. Phys.*, 98(6): 063101-063101-4.

Chazan, P., J.M. Mayor, S. Morgott, M. Mikulla, R. Kiefer, S. Muller, M. Walther, J. Braunstein and G. Weimann, 1998. High-power near-diffraction-limited tapered amplifiers at 1064 nm for optical intersatellite communications. *IEEE Photonic Tech. L.*, 10: 1542-1544.

Lim, J.J., T.M. Benson and E.C. Larkins, 2005. Design of wide-emitter single-mode laser diodes. *IEEE J. Quantum Elect.*, 41(4): 506-516.

Lim, J.J., R. MacKenzie, S. Sujecki, M. Sadeghi, S.M. Wang, Y.Q. Wei, J.S. Gustavsson, A. Larsson, P. Melanen, P. Sipila, P. Uusimaa, A.A. George, P.M. Smowton and E.C. Larkins, 2007. Simulation of double quantum well GaInNAs laser diodes. *Proceeding of the 21st Conference on Semiconductor Integrated Optoelectronics (SIOE)*. Cardiff, WALES, pp: 259-265.

Lim, J.J., S. Sujecki, L. Lang, Z.C. Zhang, D. Paboeuf, G. Pauliat, G. Lucas-Leclin, P. Georges, R.C.I. MacKenzie, P. Bream, S. Bull, K.H. Hasler, B. Sumpf, H. Wenzel, G. Erbert, B. Thestrup, P.M. Petersen, N. Michel, M. Krakowski and E.C. Larkins, 2009. Design and simulation of next-generation high-power, high-brightness laser diodes. *IEEE J. Sel. Top. Quant.*, 15: 993-1008.

Schulz, W. and R. Poprawe, 2000. Manufacturing with novel high-power diode lasers. *IEEE J. Sel. Top. Quant.*, 6: 696-705.

Steele, R., 2008. *Laser Focus World*. Retrieved from: <http://online.qmags.com/LFW1108/Default.aspx?SessionID=81697E67BEC59096E4AA81FC2&cid=798041&eid=10916>.

Tomm, J.W., A. Gerhardt, T. Elsaesser, D. Lorenzen and P. Hennig, 2002. Simultaneous quantification of strain and defects in high-power diode laser devices. *Appl. Phys. Lett.*, 81(17): 3269.

Xia, R., E.C. Larkins, I. Harrison, S.R.A. Dods, A.V. Andrianov, J. Morgan and J.P. Landesman, 2002. Mounting-induced strain threshold for the degradation of high-power AlGaAs laser bars. *IEEE Photonic Tech. L.*, 14(7): 893-895.